
Conditional Contrastive Learning for Improving Fairness in Self-Supervised Learning

Martin Q. Ma¹, Yao-Hung Hubert Tsai¹, Paul Pu Liang¹, Han Zhao²,
Kun Zhang^{1,3}, Ruslan Salakhutdinov¹, & Louis-Philippe Morency¹

¹Carnegie Mellon University ²University of Illinois at Urbana-Champaign

³Mohamed bin Zayed University of Artificial Intelligence

{qianlim, yaohungt, pliang, kunz1, rsalakhu, morency}@cs.cmu.edu
hanzhao@illinois.edu

Abstract

Contrastive self-supervised learning (SSL) learns an embedding space that maps similar data pairs closer and dissimilar data pairs farther apart. Despite its success, one issue has been overlooked: the fairness aspect of representations learned using contrastive SSL. Without mitigation, contrastive SSL techniques can incorporate sensitive information such as gender or race and cause potentially unfair predictions on downstream tasks. In this paper, we propose a Conditional Contrastive Learning (CCL) approach to improve the fairness of contrastive SSL methods. Our approach samples positive and negative pairs from distributions conditioning on the sensitive attribute, or empirically speaking, sampling positive and negative pairs from the same gender or the same race. We show that our approach provably maximizes the conditional mutual information between the learned representations of the positive pairs, and reduces the effect of the sensitive attribute by taking it as the conditional variable. On seven fairness and vision datasets, we empirically demonstrate that the proposed approach achieves state-of-the-art downstream performances compared to unsupervised baselines and significantly improves the fairness of contrastive SSL models on multiple fairness metrics.

1 Introduction

Self-supervised learning (SSL) [29], especially contrastive self-supervised learning (contrastive SSL) [9, 24], have performed well in a variety of different vision or language tasks [10, 11, 48]. Contrastive SSL frameworks [9, 24] first perform a *contrastive pre-training* by pulling together related data pairs (termed *positive pairs*) and pushing away unrelated pairs (termed *negative pairs*) in the embedding space, and then evaluate the learned representation by a *supervised fine-tuning* with labels.

However, despite the growing popularity of contrastive SSL, the potential issue of fairness in these learned representations has been understudied: **do contrastive SSL models learn fair representations, and how to mitigate potential biases?** We are particularly interested in the scenario where a potential *sensitive attribute*, such as gender or race, is already available in the dataset. We show that without care, contrastive models can incorporate information from the sensitive attributes and cause unfair predictions in downstream tasks. For example, Figure 1 illustrates a case where contrastive SSL is used to learn representations of human faces. A predominant contrastive SSL setup [9] uses two augmented views of the same image as a positive pair, and selects random images as negative pairs. In this setup, two images for the positive pair will always share the same gender since both are augmented from the same image, but two images for the negative pairs may have different genders. Therefore, a contrastive SSL model can learn to use gender-related visual attributes to push away mixed-gender images present in negative pairs. By capturing this gender-related information in

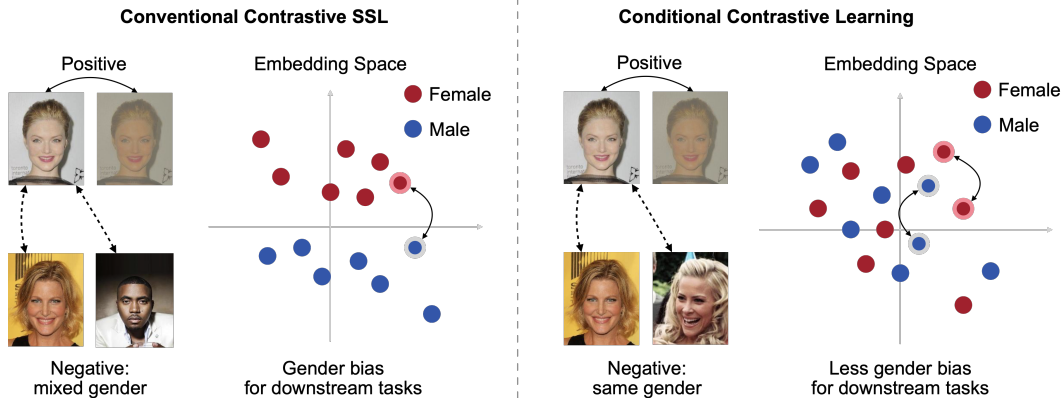


Figure 1: A demonstration of conventional contrastive SSL vs. the proposed Conditional Contrastive Learning (CCL). In conventional contrastive SSL, contrastive pre-training is performed on a mixture of female and male samples, and the model can easily pick up gender information during training and create an embedding space with gender bias for downstream tasks. On the other hand, the proposed Conditional Contrastive Learning only samples positive and negative pairs within the same gender group, making it harder for the model to leverage gender information. It can therefore create an embedding space with less gender bias. An empirical reflection of this demonstration on the CelebA dataset [38] is shown in Figure 4.

the embedding space of the learned representation, the representation can potentially cause unfair predictions when it is applied to downstream tasks.

In this paper, we empirically study this potential issue of fairness with contrastive SSL approaches, and propose a new method, Conditional Contrastive Learning (CCL), to reduce the effect from a sensitive attribute during the contrastive pre-training. We focus on scenarios where the sensitive attribute is known and our goal is to mitigate its effect. The proposed CCL approach first defines the sensitive attribute (e.g., gender) as a conditional variable and samples the positive and negative pairs from distributions conditioning on the sensitive attribute. Empirically, this can be efficiently implemented by sampling from the same sensitive attribute, i.e., from the same gender. This simple but effective approach makes it harder for the model to leverage information from the sensitive attribute to distinguish positive pairs from negative pairs. We then proved that the proposed CCL maximizes a lower bound of *conditional* mutual information between the learned representations, which explicitly excludes information from the conditional variable.

We evaluate our approach on five fairness datasets: Adult [16], German [16], COMPAS [1], Crime [16], and Law School [64], and two real-world facial datasets, CelebA [39] and UTK-Face [69]. We study the fairness of contrastive SSL with multiple fairness metrics including demographic parity, equalized odds, and equality of opportunity, with the goal of maintaining strong downstream task performances compared to unsupervised baselines.

2 Related Work

Contrastive self-supervised learning. Contrastive SSL has become successful in learning representations without labels [9, 10, 48, 50]. The aim is to learn an embedding space that pulls together positive pairs and pushes away negative pairs [11]. The representation can then be used for different downstream tasks, such as visual transfer learning [11], video action recognition [48], geolocation [48], and speech recognition [4]. Recent work relates the success of contrastive self-supervised learning to mutual information maximization [3, 3, 12, 45, 61]. Other works [45, 47, 59, 61] have shown that contrastive learning objectives can be seen as maximizing the lower bound of mutual information between the two augmented views of the same image.

Recent work in contrastive learning considers an additional conditional variable in contrastive learning to improve representation quality, such as auxiliary attributes [60], information about the downstream task [58], downstream labels [31, 32] or data embeddings [62, 65]. With the additional conditional

variables, these works extend contrastive self-supervised learning to a weakly supervised [60], semi-supervised [58], or supervised setup [32]. This work, on the other hand, primarily aims to improve the fairness (instead of representation quality) in a self-supervised setup and proposes to use the given sensitive attribute from the dataset as the conditional variable.

Some work has discussed conditional distributions or conditional mutual information for contrastive learning. Sordani et al. [57] proposes to capture more information between views in contrastive learning by decomposing mutual information into a sum of conditional mutual information, which conditions on subviews of the data (e.g., views obtained by occluding pixels of the original image). Another work [62] approximates similarity scores from conditional distributions in contrastive learning using the conditional kernel mean embedding [56]. In comparison, this work also considers conditional mutual information and conditional distributions, but aims to remove (instead of capture) effect from an additional variable, and explicitly samples from conditional distributions (rather than using variational or kernel forms) to estimate conditional mutual information.

Fair representation learning To safely deploy self-supervised models in real-world scenarios such as healthcare, legal systems, and social science, it is also necessary to recognize the role they play in shaping social biases and stereotypes. Previous work has revealed that large-scale models trained with self-supervised learning can fail with respect to certain fairness criteria, such as models generating toxic speech [20], languages denigrating to particular social groups [37, 54], among other concerns [7, 25, 36, 52]. There has been work discussing fairness in self-supervised learning via reconstruction [8], but this work is the first to discuss the fairness in contrastive self-supervised learning for visual or tabular fairness (e.g., Adult [16]) datasets.

Recent work associates contrastive learning with fair representation learning. Hong and Yang [28] improves fairness in a supervised setup by regularizing a contrastive term sampling positive pairs from the same downstream labels. [53] also considers a supervised setup with two contrastive objectives, where the positive pairs are from the same downstream label and the same sensitive attribute respectively, and the negative pairs are from different downstream labels or different sensitive attributes respectively. This work considers a self-supervised setup (instead of a supervised one), and samples both the positive and the negative pairs from the same sensitive attribute (i.e., the same gender). Recent work also proposes to maximize a lower bound of conditional mutual information (CMI) conditioning on the sensitive attribute to improve fairness, because CMI excludes information from the conditional variable [40]. Song et al. [55] considers an unsupervised setup and uses variational and adversarial objectives to estimate the CMI between the data and the representation. Gupta et al. [21] considers a supervised setup and estimates the CMI between the downstream labels and the representations. In contrast, this work considers a self-supervised setup and estimates the CMI between representation of two data views using a contrastive objective.

3 Method

In this section, we introduce our proposed Conditional Contrastive Learning (CCL) approach to improve fairness in contrastive self-supervised learning, by reducing the impact of the given sensitive attribute in the representation. We first discuss the technical background, specifically focusing on conventional setup of contrastive self-supervised learning and the corresponding InfoNCE objective [45]. We then present the CCL approach and motivate with theoretical results on why CCL can reduce the impact from the sensitive attribute.

3.1 Contrastive Self-Supervised Learning

Conventional contrastive self-supervised learning [3, 9, 24] aims to learn an embedding space that pulls together representations of similar samples (positive pairs) and push away representations of dissimilar samples (negative pairs). For example, positive pairs could be two views of the same image by stochastic data augmentation [9], while negative pairs could be two views of different images. Below, we first introduce notations of contrastive self-supervised learning, and then briefly summarize an information theory interpretation of conventional contrastive SSL [45, 61, 66], which help to both define and motivate our proposed CCL approach.

We use uppercase letters (e.g., X) to denote random variables and lowercase letters (e.g., x) to denote outcomes from the random variables. Specifically, we use x and y to denote the learned

representations after encoding two data views v_1 and v_2 created by stochastic augmentation on images, where v_1 and v_2 could be a positive (from the same image) or a negative pair (from different images):

$$x = \text{encoder}(v_1), y = \text{encoder}(v_2), \quad (1)$$

and X and Y are the corresponding random variables of representations x and y . We use P_X as the distribution of X and $D_{\text{KL}}(\cdot \parallel \cdot)$ as the Kullback–Leibler divergence between distributions.

Recent work [2, 3, 45, 61, 66] has shown that the success of contrastive SSL is related to maximizing a lower bound of mutual information shared between the representations of positive pairs. Specifically, the positive pair is sampled from the joint distribution, while the negative pairs are sampled from the product of marginal distributions. Mutual information is the KL divergence between the joint distribution and the product of marginal distributions, and optimizing a contrastive loss like Oord et al. [45] maximizes a lower bound of mutual information. Formally, the InfoNCE [45] objective is to maximize $\text{MI}(X; Y)$ as follows:

$$\text{InfoNCE} := \sup_f \mathbb{E}_{(x_i, y_i) \sim P_{X, Y}} \left[\frac{1}{n} \sum_{i=1}^n \log \frac{e^{f(x_i, y_i)}}{\frac{1}{n} \sum_{j=1}^n e^{f(x_i, y_j)}} \right] \leq D_{\text{KL}}(P_{X, Y} \parallel P_X P_Y) = \text{MI}(X; Y), \quad (2)$$

where the positive pairs $\{(x_i, y_i)\}_{i=1}^n$ are drawn from the joint distribution: $(x_i, y_i) \sim P_{X, Y}$, and the negative pairs $\{(x_i, y_{j \neq i})\}$ are drawn from the product of marginal distributions: $(x_i, y_{j \neq i}) \sim P_X P_Y$. $\text{MI}(X; Y)$ is the mutual information between X and Y . $f(x, y)$ is any similarity scoring function that considers the input (x, y) and output a similarity score. A common choice of $f(x, y)$ is the cosine similarity $f(x, y) = \cos(g(x), g(y))/\tau$, with τ being the temperature hyper-parameter and $g(\cdot)$ being a small neural network [9, 24]. At a high-level, InfoNCE performs contrastive learning by maximizing the similarity for the positive pairs and minimizing the similarity for the negative pairs. As shown in (2), InfoNCE is a lower bound of $\text{MI}(X; Y)$, and several works [2, 61] have shown that maximizing lower bounds of $\text{MI}(X; Y)$ leads to better representations for downstream tasks.

3.2 Conditional Contrastive Learning

Our proposed method, Conditional Contrastive Learning (CCL), differs from conventional contrastive SSL, by taking positive pairs and negative pairs from the distributions conditioning on a sensitive attribute referred as Z . Our CCL approach reduces information from the sensitive attribute Z by taking Z as the conditional variable between X and Y . We focus on scenarios where Z is readily available in the dataset (e.g., gender, race or age), following the practice of previous work on fairness [41, 55]. Now we present the proposed **Conditional Contrastive Learning** objective:

$$\text{CCL} := \sup_f \mathbb{E}_{z \sim P_Z} \left[\mathbb{E}_{(x_i, y_i) \sim P_{X, Y|z}} \left[\frac{1}{n} \sum_{i=1}^n \log \frac{e^{f(x_i, y_i)}}{\frac{1}{n} \sum_{j=1}^n e^{f(x_i, y_j)}} \right] \right] \quad (3)$$

where the positive pairs $\{(x_i, y_i)\}_{i=1}^n$ represent samples drawn from the *conditional* joint distribution: $(x_i, y_i) \sim P_{X, Y|z}$, while the negative pairs $\{(x_i, y_{j \neq i})\}$ represent samples drawn from the product of *conditional* marginal distributions: $(x_i, y_{j \neq i}) \sim P_{X|z} P_{Y|z}$. The score function is $f(x, y) = \cos(g(x), g(y))/\tau$, same as (2). The difference between CCL and InfoNCE can be phrased as follows: CCL first samples $z \sim Z$, and then samples positive and negative pairs from $P_{X, Y|z}$ and $P_{X|z} P_{Y|z}$, respectively. InfoNCE, on the contrary, directly samples from $P_{X, Y}$ and $P_X P_Y$. Sampling from conditional distributions in CCL means that all positive and negative pairs share the same outcome z of the sensitive attribute Z . Empirically, we could implement this by first sampling from the sensitive attribute (e.g., the gender), and then sampling positive and negative pairs from the same outcome of the sensitive attribute (i.e., the same gender). While we focus on InfoNCE for this paper, we should note that CCL can also be applied to other contrastive objective functions, especially divergence-based, such as Donsker-Varadhan [15], Jensen-Shannon [6], or Wasserstein [46], by applying the aforementioned sampling procedure to get the positive and negative pairs and plugging them in the contrastive objectives.

3.3 Theoretical Motivation

In this section, we provide the theoretical motivation for our CCL method. In particular, we are interested in understanding why our method can reduce the information related to the sensitive

attribute Z . Due to space limit, we defer detailed proofs of Equations (4) and (5) to Appendix Section A. Recall that InfoNCE is maximizing a lower bound of $D_{\text{KL}}(P_{X,Y} \| P_X P_Y)$ as shown in (2). Similarly, our CCL method aims to maximize the divergence between $P_{XY|z}$ and $P_{X|z}P_{Y|z}$ for all $z \sim P_Z$, leading to a connection with conditional mutual information $\text{MI}(X; Y|Z)$. First, we define conditional mutual information (CMI):

$$\text{CMI}(X; Y|Z) := \mathbb{E}_{z \sim Z} [D_{\text{KL}}(P_{X,Y|Z=z} \| P_{X|Z=z}P_{Y|Z=z})] = \int_Z D_{\text{KL}}(P_{X,Y|Z} \| P_{X|Z}P_{Y|Z}) dP_Z, \quad (4)$$

which measures the expected mutual information of X and Y given Z . Intuitively, $\text{CMI}(X; Y|Z)$ measures the averaged shared information by X and Y but exclude the effect from Z [40]. This is because conditioning $Z = z$ means taking $Z = z$ as known and, therefore, ignoring the effect of Z [44]. By ignoring the effect of Z , $\text{CMI}(X; Y|Z)$ explicitly excludes the information from Z when measuring the shared information between X and Y .

Next, we show our main theoretical result, that the proposed CCL objective is a lower bound of the conditional mutual information $\text{CMI}(X; Y|Z)$:

$$\text{CCL} \leq D_{\text{KL}}(P_{X,Y} \| \mathbb{E}_{P_Z} [P_{X|Z}P_{Y|Z}]) = \text{Weak-CMI}(X; Y|Z) \leq \text{CMI}(X; Y|Z), \quad (5)$$

where $\text{Weak-CMI}(X; Y|Z)$ is the KL-divergence between $P_{X,Y}$ and $\mathbb{E}_{P_Z} [P_{X|Z}P_{Y|Z}]$. This notion has been used to achieve the so-called weak-conditional independence [14, 18, 19]. We have the weak conditional independence between X and Y given Z when $\text{Weak-CMI}(X; Y|Z) = 0$. First, $\text{Weak-CMI}(X; Y|Z) = 0$ is a necessary but not sufficient condition for $\text{CMI}(X; Y|Z) = 0$, suggesting that conditional independence implies weak conditional independence. For example, if X , Y , and Z are pairwise independent but jointly dependent, $\text{Weak-CMI}(X; Y|Z) = 0$ but $\text{CMI}(X; Y|Z)$ may not be zero. Although weak conditional independence does not fully characterize conditional independence, it has been shown to be widely useful in practice. For instance, testing weak conditional independence can be simpler and more powerful than the original conditional independence test [68]. Our approach benefits from the notion of weak conditional independence in similar ways. Also, we prove that $\text{Weak-CMI}(X; Y|Z)$ is a lower bound of $\text{CMI}(X; Y|Z)$ and can be seen as a more ‘‘conservative’’ measurement of $\text{CMI}(X; Y|Z)$, capturing only part of information in $\text{CMI}(X; Y|Z)$.

Why CCL may work? Two main observations can be deduced from the theoretical result. The first observation relates to *fairness*, while the second observation relates to *representation quality*. For the first observation concerning fairness, we draw a Venn diagram of $\text{CMI}(X; Y|Z)$ to illustrate why the impact of Z is reduced. As shown in Figure 2, $\text{CMI}(X; Y|Z)$ explicitly excludes information from Z [40]. Since CCL is the lower bound of $\text{CMI}(X; Y|Z)$, the impact of Z will be reduced as we optimize CCL. For the second observation about representation quality, maximizing CCL results in maximizing a lower bound of $\text{CMI}(X; Y|Z)$ between the representation X of data view V_1 and representation Y of data view V_2 given Z . Previous work such [27, 45, 61] has shown that maximizing the information shared between X and Y can produce a good embedding space that has high *representation quality* for downstream tasks.

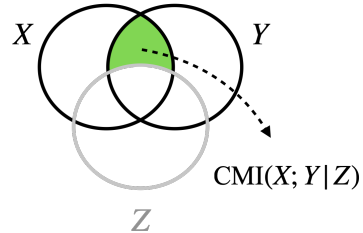


Figure 2: Venn diagram of $\text{CMI}(X; Y|Z)$ (the green section).

4 Experiments

We evaluate the proposed Conditional Contrastive Learning on several tasks, summarized in Table 1. We experiment with five fairness datasets: Adult [16], Compas [1], Crime [16], German [16], and Law School [64], and two facial datasets: CelebA [38] and UTKFace [69]. The sensitive attributes for each experiment are also summarized in Table 1. The corresponding sensitive attribute for each dataset is used as the conditioning variable for the proposed CCL. We evaluate on prediction accuracy (all tasks being binary predictions) and three fairness metrics (in the form of distance): Demographic Parity (Δ_{DP}), Equalized Odds (Δ_{EO}), and Equality of Opportunity ($\Delta_{EO_{PP}}$). We include all implementation details, including hyperparameters, datasets and source code in Appendix Section B.

4.1 Fairness Criteria

Table 1: Details of datasets, the chosen sensitive attributes, and the corresponding prediction tasks. There are three prediction task for CelebA: attractiveness, weary hair, and smiling.

Datasets	Type	Number of Samples	Sensitive Attribute	Prediction Task(s)
Adult [16]	Tabular	48,842	Gender	Income level
Compas [1]	Tabular	5,278	Race	Recidivism
Crime [16]	Tabular	1,994	Race	Crime level
German [16]	Tabular	1,000	Age	Credit approval
Law School [64]	Tabular	36,022	Race	Exam result
UTKFace [69]	Vision	23,708	Race	Age
CelebA [38]	Vision	202,599	Gender	Multiple

We use three types of fairness metrics: the demographic parity (DP [17]) distance Δ_{DP} [41], equalized odds (EO [22]) distance Δ_{EO} [55], and the equality of opportunity (EO_{PP} [22]) distance $\Delta_{EO_{PP}}$ [55]. Given the data X , the sensitive attribute Z indicating group information, the ground truth downstream task label l , and the label prediction from the model \hat{l} , the Δ_{DP} calculates the expected difference (in absolute value) in model predictions between two groups: $\Delta_{DP} = |\mathbb{P}\{\hat{l} = 1|Z = 0\} - \mathbb{P}\{\hat{l} = 1|Z = 1\}|$. The second metric, Δ_{EO} , calculates the sum of the expected difference (in absolute value) of the True Positive Rate and the False Positive Rate of the model predictions between two groups: $\Delta_{EO} = |\mathbb{P}\{\hat{l} = 1|Z = 0, l = 1\} - \mathbb{P}\{\hat{l} = 1|Z = 1, l = 1\}| + |\mathbb{P}\{\hat{l} = 1|Z = 0, l = 0\} - \mathbb{P}\{\hat{l} = 1|Z = 1, l = 0\}|$. As a relaxation of Δ_{EO} , $\Delta_{EO_{PP}}$ calculates the expected difference (in absolute value) of only the True Positive Rate of the model predictions between two groups: $\Delta_{EO_{PP}} = |\mathbb{P}\{\hat{l} = 1|Z = 0, l = 1\} - \mathbb{P}\{\hat{l} = 1|Z = 1, l = 1\}|$. Δ_{DP} , Δ_{EO} , $\Delta_{EO_{PP}}$ range from 0 to 1, and a smaller distance is desirable. $\Delta_{DP} = 0$ corresponds to the statistical independence of the sensitive attribute Z and the prediction \hat{l} , and $\Delta_{EO} = 0$ corresponds to the conditional independence of Z and \hat{l} given the true label l . Intuitively, for example, $\Delta_{DP} = 0$ suggests that members of different groups (e.g., female and male) have the same chance of receiving a favorable prediction ($l = 1$).

4.2 Experimental Methodology

We follow the setup from the contrastive SSL learning literature [9, 24], which contains two stages: contrastive pre-training and supervised fine-tuning. We use the SimCLR framework [9]. In contrastive pre-training, we train an encoder without any labels. In the supervised fine-tuning stage, we freeze the encoder and fine-tune an additional small network with the downstream labels. We then evaluate the fine-tuned representations on the test splits of the corresponding datasets. For fairness datasets, we use a three-layer neural network with hidden dimension 100 as the encoder and a linear layer as the fine-tuning network. For vision datasets, we use a ResNet-50 [23] as the encoder and a two-layer network as the fine-tuning network. There are two types of baselines: unsupervised and SSL baselines. Unsupervised baselines include models dedicated for improving fairness in unsupervised representations. The SSL baseline includes implementations of the InfoNCE loss on SimCLR. We did not include supervised fair representation models, as they often require labels and sensitive attributes to be available at the same time, which is not our case.

4.3 Fairness Dataset Experiments

Implementation Details. The self-supervised baseline, SimCLR [45], and the unsupervised baseline, LCIFR [51] are re-implemented based on Ruoss et al. [51]. To stochastically augment tabular features (e.g., age, education, occupation, etc in Adult [16] dataset) and create data views similar to Chen et al. [9], we first standardize each tabular feature, and then use noise vectors from an isotropic Gaussian to perturb the features. Each dataset uses one separate Gaussian, and σ of the Gaussian is treated as a hyper-parameter for different datasets. Then we feed the augmented views to the encoder, and then use the output of the encoder to estimate our proposed CCL.

Table 2: Accuracies and fairness results on five fairness datasets. Details of these baselines are in Appendix Section B. Best results are in bold. CCL has better downstream accuracy than existing unsupervised and self-supervised baselines in four datasets, and exhibits better fairness measurements in 11 out of 18 results.

	Model	Accuracy (%) (\uparrow)	Δ_{DP} (\downarrow)	Δ_{EO} (\downarrow)	$\Delta_{EO_{PP}}$ (\downarrow)
ADULT	Unsupervised				
	– LAFTR [41]	84.0	0.163	0.030	0.026
	– Ragonesi et al. [49]	85.0	-	0.030	-
	– DTM [35]	71.6	-	0.050	-
	– FNF [5]	80.0	0.110	-	-
	Self-Supervised				
	– SimCLR [9]	83.1	0.210	0.410	0.320
– FairMixRep [8]	85.0	0.172	-	-	
– CCL (Ours)	85.4	0.110	0.070	0.090	
COMPAS	Unsupervised				
	– DTM [35]	66.0	-	0.200	-
	– FNF [5]	65.0	0.240	-	-
	Self-Supervised				
	– SimCLR [9]	71.2	0.103	0.227	0.134
– CCL (Ours)	71.0	0.080	0.132	0.081	
CRIME	Unsupervised				
	– LCIFR [51]	84.4	0.443	0.314	0.212
	– FNF [5]	82.5	0.540	-	-
	Self-Supervised				
	– SimCLR [9]	82.1	0.502	0.530	0.383
– CCL (Ours)	82.6	0.211	0.224	0.183	
GERMAN	Unsupervised				
	– LCIFR [51]	73.1	0.102	0.080	0.063
	– Ragonesi et al. [49]	74.0	-	0.060	-
	Self-Supervised				
	– FairMixRep [8]	71.8	0.089	-	-
– SimCLR [9]	72.5	0.250	0.382	0.195	
– CCL (Ours)	74.3	0.083	0.128	0.062	
LAW SCHOOL	Unsupervised				
	– LCIFR [51]	84.4	0.110	0.180	0.070
	– FNF [5]	84.6	0.050	-	-
	Self-Supervised				
	– SimCLR [9]	83.6	0.086	0.212	0.110
– CCL (Ours)	84.8	0.051	0.153	0.056	

Results. Table 2 shows the results on accuracy and fairness metrics for both unsupervised and self-supervised methods. First, we observe that self-supervised SimCLR and CCL have strong downstream prediction results close to or better than the state-of-the-art baselines in Adult, Compas, German and the Law School datasets. Next, looking at the fairness measurements, we observe that the SimCLR baseline performs significantly worse than unsupervised baselines, sometimes two to three times higher (Δ_{DP} in Adult, Δ_{EO} in German, and $\Delta_{EO_{PP}}$ in Adult), confirming our earlier concern that contrastive self-supervised learning will produce highly unfair predictions without bias mitigation. The proposed CCL is much better than SimCLR and very competitive compared to other unsupervised baselines, in terms of fairness criteria: the average improvement over five datasets from SimCLR to CCL is 12.28% on Δ_{DP} , 21.08% on Δ_{EO} , and 13.43% on $\Delta_{EO_{PP}}$.

Effect of hyper-parameters on downstream performances. We study two important hyper-parameters using the Adult dataset: the σ of the Gaussian noise and the temperature τ in Equation 3. The Gaussian noise controls the level of data augmentation, and τ smooths the distribution of the score output of the encoder. Both will influence the representation quality in contrastive learning. We use $\tau \in [0.001, 1]$; and $\sigma \in [0.001, 2]$. The results are shown in Figure 3. We observe that a mid-range

$\tau = 0.25$ achieves the best results. The prediction accuracy begins to increase drastically as τ goes from 0.001, tops at $\tau = 0.25$, and start decreasing slightly from $\tau = 0.5$. Next, for the noise level, we observe that a small σ ranging from 0.001 to 0.75 achieves similar results (around or above 84%), peaks at $\sigma = 0.25$, and then degrades fast after 0.75. This suggests that a mid-range temperature ($\tau = 0.25$) to smooth the similarity score distribution [26], and a mild noise augmentation ($\sigma = 0.25$) to the tabular data help the most in representation learning.

Effect of hyper-parameters on fairness.

We also study the effect of σ and τ in terms of fairness criteria: Δ_{DP} , Δ_{EO} , and $\Delta_{EO_{PP}}$. Overall, a similar trend occurs for three criteria: a large noise ($\sigma > 0.75$) and a large temperature ($\tau > 0.5$) generates the worst representation in terms of fairness metrics ($\Delta_{DP} > 0.2$, $\Delta_{EO} > 0.3$ and $\Delta_{EO_{PP}} > 0.3$). On the other hand, a large noise ($\sigma > 0.75$) and a medium-to-small temperature ($\tau < 0.5$) generates the best results on fairness, but in these cases the representation performs badly on downstream tasks. The right trade-off between representation power and fairness we found is $\tau \in [0.1, 0.5]$ and $\sigma \in [0.001, 0.25]$. The results suggest that a larger noise and a mid-range temperature may help remove bias information.

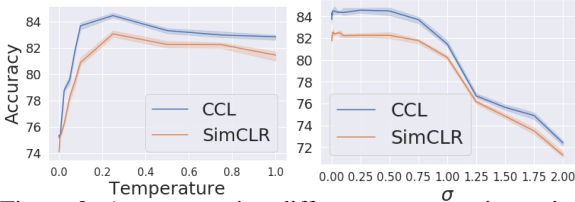


Figure 3: Accuracy using different augmentation noise level σ and temperature τ . Left: Varying temperature τ on prediction accuracy, $\sigma = 0.25$. Right: Varying augmentation noise σ on prediction accuracy, $\tau = 0.25$. A mid-range $\tau = 0.25$ and a mild noise level $\sigma = 0.25$ helps the most for learning strong representations.

4.4 Vision Dataset Experiments

We implement the baseline SimCLR by following Chen et al. [9] and using the augmentations resize-and-crop, color jitter and horizontal flip. We evaluate on the prediction tasks specified in Table 1 (age prediction for UTKFace, and attractiveness / weary hair / smiling prediction for CelebA). The sensitive attribute for UTKFace is race, and gender for CelebA. The results are in Table 2. We observe that the proposed CCL both outperforms unsupervised baselines and the self-supervised SimCLR baseline on the prediction tasks. The CCL also achieves much better fairness criteria than the SimCLR baseline, producing much lower Δ_{DP} , Δ_{EO} , and $\Delta_{EO_{PP}}$ in all four tasks across two datasets.

We also plot the embedding spaces of SimCLR and CCL using t-SNE [63]. The visualization is in Figure 4. The embeddings of female and male group samples are clearly separated in SimCLR, making it easy for downstream fine-tuning models to pick up gender information and produce unfair predictions. On the other hand, for the embedding from CCL it is much hard to separate two groups, making it hard for models to leverage gender information from the representation.

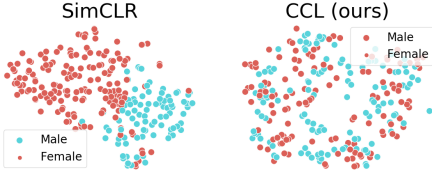


Figure 4: T-SNE embeddings of conventional contrastive SSL (SimCLR, left) vs. Conditional Contrastive Learning (ours, right). Gender groups are visually inseparable in the CCL (right) compared to conventional contrastive SSL (left), suggesting an embedding with less gender biases.

Table 3: Fairness criteria on contrastive SSL vs. supervised counterpart. Contrastive SSL has much higher level of fairness differences based on the three metrics.

	Accuracy	$\Delta_{DP} (\downarrow)$	$\Delta_{EO} (\downarrow)$	$\Delta_{EO_{PP}} (\downarrow)$
Supervised	80.4	0.214	0.186	0.080
Contrastive SSL	80.1	0.355	0.541	0.310

Contrastive SSL performs worse on fairness than supervised methods. To study whether contrastive SSL models perform better or worse on fairness criteria than a supervised counterpart, we train two ResNet-18 models [23], one with contrastive pre-training then fine-tuning [24], and one with supervised training. Both models

have the same architecture and training hyperparameters. From Table 3, given similar performance, contrastive SSL has significantly larger fairness differences, suggesting that contrastive SSL can

produce downstream predictions that perform much worse on fairness criteria than its supervised counterpart.

Table 4: Accuracies and fairness results on two vision datasets with four prediction tasks. Best results are bold. CCL has better downstream accuracy in all four tasks, and exhibits better or close-to-the-best fairness measurements in 11 out of 12 results.

	Model	Accuracy (%) (\uparrow)	Δ_{DP} (\downarrow)	Δ_{EO} (\downarrow)	$\Delta_{EO_{PP}}$ (\downarrow)
CELEBA ATTRACTIVE	Unsupervised				
	– MFD [30]	80.2	-	0.050	-
	– Balunovic et al. [5]	79.4	-	0.238	-
	– Morales et al. [42]	77.7	-	0.070	-
	Self-Supervised				
	– SimCLR [9]	81.7	0.277	0.212	0.110
– CCL (Ours)	82.1	0.202	0.101	0.048	
CELEBA WAVY HAIR	Unsupervised				
	– FactorVAE [33]	64.5	-	0.388	0.288
	– FFVAE [13]	61.0	-	0.211	0.154
	Self-Supervised				
	– SimCLR [9]	67.7	0.403	0.355	0.210
	– CCL (Ours)	67.7	0.202	0.189	0.102
CELEBA SMILE	Unsupervised				
	– Morales et al. [42]	88.4	-	0.060	-
	Self-Supervised				
	– SimCLR [9]	89.3	0.102	0.142	0.078
– CCL (Ours)	89.7	0.086	0.060	0.053	
UTKFACE GENDER	Unsupervised				
	– AD [67]	74.7	-	0.204	-
	– MFD [30]	74.7	-	0.178	-
	Self-Supervised				
	– SimCLR [9]	78.0	0.335	0.421	0.287
	– CCL (Ours)	78.5	0.191	0.156	0.089

5 Discussion, Limitations and Social Impact

We introduce Conditional Contrastive Learning (CCL) which samples positive and negative pairs from distributions conditioning on the sensitive attribute to remove its effect, and thus improving fairness in self-supervised learning. By conditioning on the sensitive attribute, the positive and negative pairs come from the same subgroup, making it harder for the model to leverage gender-related information. We prove that CCL is a lower bound of conditional mutual information, and optimizing it leads to learning strong representations for downstream tasks while reducing the information from the sensitive attribute. Empirically, we show that CCL significantly improves the fairness of conventional contrastive models, while achieving SOTA downstream performances compared to both contrastive SSL and other unsupervised baselines.

One important future work direction, and a limitation of this work, is to study the scenario the sensitive information is unknown or partially known. It could be addressed by using other auxiliary attributes (e.g., image annotations or captions) in the datasets that are highly relevant to the sensitive attributes, or first train a separate model to capture bias features and then train the main model by learning features orthogonal to the bias feature. Another important problem is to remove the effect of multiple sensitive attributes simultaneously, which may be addressed by using a joint distribution of multiple sensitive attributes. If there are too many sensitive attributes, we can perform a dimensional reduction. For the social impact, CCL may bring a positive impact by removing gender, race, or identity information from representations. The potential negative impact is that this method could be intentionally used to remove information that should be available and included in the representation, for example, gender information in a model for medical diagnosis.

References

- [1] J. Angwin, J. Larson, S. Mattu, and L. Kirchner. Machine bias. *ProPublica*, May, 23(2016): 139–159, 2016.
- [2] S. Arora, H. Khandeparkar, M. Khodak, O. Plevrakis, and N. Saunshi. A theoretical analysis of contrastive unsupervised representation learning. *arXiv preprint arXiv:1902.09229*, 2019.
- [3] P. Bachman, R. D. Hjelm, and W. Buchwalter. Learning representations by maximizing mutual information across views. *arXiv preprint arXiv:1906.00910*, 2019.
- [4] A. Baeovski, H. Zhou, A. Mohamed, and M. Auli. wav2vec 2.0: A framework for self-supervised learning of speech representations. *arXiv preprint arXiv:2006.11477*, 2020.
- [5] M. Balunovic, A. Ruoss, and M. Vechev. Fair normalizing flows. In *International Conference on Learning Representations*, 2021.
- [6] M. I. Belghazi, A. Baratin, S. Rajeshwar, S. Ozair, Y. Bengio, A. Courville, and D. Hjelm. Mutual information neural estimation. In *International conference on machine learning*, pages 531–540. PMLR, 2018.
- [7] S. L. Blodgett, S. Barocas, H. Daumé III, and H. Wallach. Language (technology) is power: A critical survey of “bias” in nlp. In *Proceedings of the 58th Annual Meeting of the Association for Computational Linguistics*, pages 5454–5476, 2020.
- [8] S. Chakraborty, E. Verma, S. Sahoo, and J. Datta. Fairmixrep: Self-supervised robust representation learning for heterogeneous data with fairness constraints. In *2020 International Conference on Data Mining Workshops (ICDMW)*, pages 458–463. IEEE, 2020.
- [9] T. Chen, S. Kornblith, M. Norouzi, and G. Hinton. A simple framework for contrastive learning of visual representations. In *International conference on machine learning*, pages 1597–1607. PMLR, 2020.
- [10] T. Chen, S. Kornblith, K. Swersky, M. Norouzi, and G. Hinton. Big self-supervised models are strong semi-supervised learners. *arXiv preprint arXiv:2006.10029*, 2020.
- [11] X. Chen, S. Xie, and K. He. An empirical study of training self-supervised vision transformers. *arXiv preprint arXiv:2104.02057*, 2021.
- [12] Z. Chi, L. Dong, F. Wei, N. Yang, S. Singhal, W. Wang, X. Song, X.-L. Mao, H. Huang, and M. Zhou. InfoXlm: An information-theoretic framework for cross-lingual language model pre-training. *arXiv preprint arXiv:2007.07834*, 2020.
- [13] E. Creager, D. Madras, J.-H. Jacobsen, M. Weis, K. Swersky, T. Pitassi, and R. Zemel. Flexibly fair representation learning by disentanglement. In *International conference on machine learning*, pages 1436–1445. PMLR, 2019.
- [14] J. Daudin. Partial association measures and an application to qualitative regression. *Biometrika*, 67(3):581–590, 1980.
- [15] M. D. Donsker and S. S. Varadhan. Asymptotic evaluation of certain markov process expectations for large time, i. *Communications on Pure and Applied Mathematics*, 28(1):1–47, 1975.
- [16] D. Dua and C. Graff. UCI machine learning repository, 2017. URL <http://archive.ics.uci.edu/ml>.
- [17] M. Feldman, S. A. Friedler, J. Moeller, C. Scheidegger, and S. Venkatasubramanian. Certifying and removing disparate impact. In *proceedings of the 21th ACM SIGKDD international conference on knowledge discovery and data mining*, pages 259–268, 2015.
- [18] K. Fukumizu, F. R. Bach, and M. I. Jordan. Dimensionality reduction for supervised learning with reproducing kernel hilbert spaces. *Journal of Machine Learning Research*, 5(Jan):73–99, 2004.
- [19] K. Fukumizu, A. Gretton, X. Sun, and B. Schölkopf. Kernel measures of conditional dependence. In *NIPS*, volume 20, pages 489–496, 2007.
- [20] S. Gehman, S. Gururangan, M. Sap, Y. Choi, and N. A. Smith. Realtotoxicityprompts: Evaluating neural toxic degeneration in language models. In *Proceedings of the 2020 Conference on Empirical Methods in Natural Language Processing: Findings*, pages 3356–3369, 2020.

- [21] U. Gupta, A. Ferber, B. Dilkina, and G. Ver Steeg. Controllable guarantees for fair outcomes via contrastive information estimation. *arXiv preprint arXiv:2101.04108*, 2021.
- [22] M. Hardt, E. Price, and N. Srebro. Equality of opportunity in supervised learning. *arXiv preprint arXiv:1610.02413*, 2016.
- [23] K. He, X. Zhang, S. Ren, and J. Sun. Deep residual learning for image recognition. In *Proceedings of the IEEE conference on computer vision and pattern recognition*, pages 770–778, 2016.
- [24] K. He, H. Fan, Y. Wu, S. Xie, and R. Girshick. Momentum contrast for unsupervised visual representation learning. In *Proceedings of the IEEE/CVF Conference on Computer Vision and Pattern Recognition*, pages 9729–9738, 2020.
- [25] D. Hendrycks, C. Burns, S. Basart, A. Critch, J. Li, D. Song, and J. Steinhardt. Aligning AI with shared human values. In *International Conference on Learning Representations*, 2021. URL https://openreview.net/forum?id=dNy_RKzJacY.
- [26] G. Hinton, O. Vinyals, J. Dean, et al. Distilling the knowledge in a neural network. *arXiv preprint arXiv:1503.02531*, 2(7), 2015.
- [27] R. D. Hjelm, A. Fedorov, S. Lavoie-Marchildon, K. Grewal, P. Bachman, A. Trischler, and Y. Bengio. Learning deep representations by mutual information estimation and maximization. *arXiv preprint arXiv:1808.06670*, 2018.
- [28] Y. Hong and E. Yang. Unbiased classification through bias-contrastive and bias-balanced learning. *Advances in Neural Information Processing Systems*, 34, 2021.
- [29] L. Jing and Y. Tian. Self-supervised visual feature learning with deep neural networks: A survey. *IEEE Transactions on Pattern Analysis and Machine Intelligence*, 2020.
- [30] S. Jung, D. Lee, T. Park, and T. Moon. Fair feature distillation for visual recognition. In *Proceedings of the IEEE/CVF Conference on Computer Vision and Pattern Recognition*, pages 12115–12124, 2021.
- [31] M. Kang and J. Park. Contragan: Contrastive learning for conditional image generation. *Advances in Neural Information Processing Systems*, 33:21357–21369, 2020.
- [32] P. Khosla, P. Teterwak, C. Wang, A. Sarna, Y. Tian, P. Isola, A. Maschinot, C. Liu, and D. Krishnan. Supervised contrastive learning. *arXiv preprint arXiv:2004.11362*, 2020.
- [33] H. Kim and A. Mnih. Disentangling by factorising. In *International Conference on Machine Learning*, pages 2649–2658. PMLR, 2018.
- [34] D. P. Kingma and J. Ba. Adam: A method for stochastic optimization. *arXiv preprint arXiv:1412.6980*, 2014.
- [35] J. Lee, Y. Bu, P. Sattigeri, R. Panda, G. Wornell, L. Karlinsky, and R. Feris. A maximal correlation approach to imposing fairness in machine learning. *arXiv preprint arXiv:2012.15259*, 2020.
- [36] P. P. Liang, I. M. Li, E. Zheng, Y. C. Lim, R. Salakhutdinov, and L.-P. Morency. Towards debiasing sentence representations. In *Proceedings of the 58th Annual Meeting of the Association for Computational Linguistics*, pages 5502–5515, 2020.
- [37] P. P. Liang, C. Wu, L.-P. Morency, and R. Salakhutdinov. Towards understanding and mitigating social biases in language models. In *ICML*, 2021.
- [38] Z. Liu, P. Luo, X. Wang, and X. Tang. Deep learning face attributes in the wild. In *Proceedings of the IEEE international conference on computer vision*, pages 3730–3738, 2015.
- [39] Z. Liu, P. Luo, X. Wang, and X. Tang. Deep learning face attributes in the wild. In *Proceedings of International Conference on Computer Vision (ICCV)*, December 2015.
- [40] D. J. MacKay, D. J. Mac Kay, et al. *Information theory, inference and learning algorithms*. Cambridge university press, 2003.
- [41] D. Madras, E. Creager, T. Pitassi, and R. Zemel. Learning adversarially fair and transferable representations. In *International Conference on Machine Learning*, pages 3384–3393. PMLR, 2018.

- [42] A. Morales, J. Fierrez, R. Vera-Rodriguez, and R. Tolosana. Sensitivenets: Learning agnostic representations with application to face images. *IEEE Transactions on Pattern Analysis and Machine Intelligence*, 43(6):2158–2164, 2020.
- [43] X. Nguyen, M. J. Wainwright, and M. I. Jordan. Estimating divergence functionals and the likelihood ratio by convex risk minimization. *IEEE Transactions on Information Theory*, 56(11):5847–5861, 2010.
- [44] J. Novovičová, P. Somol, M. Haindl, and P. Pudil. Conditional mutual information based feature selection for classification task. In *Iberoamerican Congress on Pattern Recognition*, pages 417–426. Springer, 2007.
- [45] A. v. d. Oord, Y. Li, and O. Vinyals. Representation learning with contrastive predictive coding. *arXiv preprint arXiv:1807.03748*, 2018.
- [46] S. Ozair, C. Lynch, Y. Bengio, A. v. d. Oord, S. Levine, and P. Sermanet. Wasserstein dependency measure for representation learning. *arXiv preprint arXiv:1903.11780*, 2019.
- [47] B. Poole, S. Ozair, A. Van Den Oord, A. Alemi, and G. Tucker. On variational bounds of mutual information. In *International Conference on Machine Learning*, pages 5171–5180. PMLR, 2019.
- [48] A. Radford, J. W. Kim, C. Hallacy, A. Ramesh, G. Goh, S. Agarwal, G. Sastry, A. Askell, P. Mishkin, J. Clark, et al. Learning transferable visual models from natural language supervision. *arXiv preprint arXiv:2103.00020*, 2021.
- [49] R. Ragonesi, R. Volpi, J. Cavazza, and V. Murino. Learning unbiased representations via mutual information backpropagation. In *Proceedings of the IEEE/CVF Conference on Computer Vision and Pattern Recognition*, pages 2729–2738, 2021.
- [50] M. Rivière, A. Joulin, P.-E. Mazaré, and E. Dupoux. Unsupervised pretraining transfers well across languages. In *ICASSP 2020-2020 IEEE International Conference on Acoustics, Speech and Signal Processing (ICASSP)*, pages 7414–7418. IEEE, 2020.
- [51] A. Ruoss, M. Balunović, M. Fischer, and M. Vechev. Learning certified individually fair representations. *arXiv preprint arXiv:2002.10312*, 2020.
- [52] M. Sap, S. Gabriel, L. Qin, D. Jurafsky, N. A. Smith, and Y. Choi. Social bias frames: Reasoning about social and power implications of language. In *Proceedings of the 58th Annual Meeting of the Association for Computational Linguistics*, pages 5477–5490, 2020.
- [53] A. Shen, X. Han, T. Cohn, T. Baldwin, and L. Frermann. Contrastive learning for fair representations. *arXiv preprint arXiv:2109.10645*, 2021.
- [54] E. Sheng, K.-W. Chang, P. Natarajan, and N. Peng. The woman worked as a babysitter: On biases in language generation. In *Proceedings of the 2019 Conference on Empirical Methods in Natural Language Processing and the 9th International Joint Conference on Natural Language Processing (EMNLP-IJCNLP)*, pages 3398–3403, 2019.
- [55] J. Song, P. Kalluri, A. Grover, S. Zhao, and S. Ermon. Learning controllable fair representations. In *The 22nd International Conference on Artificial Intelligence and Statistics*, pages 2164–2173. PMLR, 2019.
- [56] L. Song, K. Fukumizu, and A. Gretton. Kernel embeddings of conditional distributions: A unified kernel framework for nonparametric inference in graphical models. *IEEE Signal Processing Magazine*, 30(4):98–111, 2013.
- [57] A. Sordoni, N. Dziri, H. Schulz, G. Gordon, P. Bachman, and R. T. Des Combes. Decomposed mutual information estimation for contrastive representation learning. In *International Conference on Machine Learning*, pages 9859–9869. PMLR, 2021.
- [58] Y. Tian, C. Sun, B. Poole, D. Krishnan, C. Schmid, and P. Isola. What makes for good views for contrastive learning? *arXiv preprint arXiv:2005.10243*, 2020.
- [59] C. Tosh, A. Krishnamurthy, and D. Hsu. Contrastive learning, multi-view redundancy, and linear models. In *Algorithmic Learning Theory*, pages 1179–1206. PMLR, 2021.
- [60] Y.-H. H. Tsai, T. Li, W. Liu, P. Liao, R. Salakhutdinov, and L.-P. Morency. Integrating auxiliary information in self-supervised learning. *arXiv preprint arXiv:2106.02869*, 2021.
- [61] Y.-H. H. Tsai, Y. Wu, R. Salakhutdinov, and L.-P. Morency. Self-supervised learning from a multi-view perspective. In *ICLR*, 2021.

- [62] Y.-H. H. Tsai, T. Li, M. Q. Ma, H. Zhao, K. Zhang, L.-P. Morency, and R. Salakhutdinov. Conditional contrastive learning with kernel. *arXiv preprint arXiv:2202.05458*, 2022.
- [63] L. Van der Maaten and G. Hinton. Visualizing data using t-sne. *Journal of machine learning research*, 9(11), 2008.
- [64] L. F. Wightman. *LSAC national longitudinal bar passage study*. Law School Admission Council, 1998.
- [65] M. Wu, M. Mosse, C. Zhuang, D. Yamins, and N. Goodman. Conditional negative sampling for contrastive learning of visual representations. *arXiv preprint arXiv:2010.02037*, 2020.
- [66] M. Wu, C. Zhuang, M. Mosse, D. Yamins, and N. Goodman. On mutual information in contrastive learning for visual representations. *arXiv preprint arXiv:2005.13149*, 2020.
- [67] B. H. Zhang, B. Lemoine, and M. Mitchell. Mitigating unwanted biases with adversarial learning. In *Proceedings of the 2018 AAAI/ACM Conference on AI, Ethics, and Society*, pages 335–340, 2018.
- [68] Q. Zhang, S. Filippi, S. Flaxman, and D. Sejdinovic. Feature-to-feature regression for a two-step conditional independence test. 2017.
- [69] Z. Zhang, Y. Song, and H. Qi. Age progression/regression by conditional adversarial autoencoder. In *Proceedings of the IEEE conference on computer vision and pattern recognition*, pages 5810–5818, 2017.

A Theoretical Analysis

This section provides the theoretical analysis of Equations (4) and (5) in the main text. The full set of assumptions of all theoretical results and complete proofs of all theoretical results are presented below.

A.1 Useful lemmas

We first present the following lemmas, which will be later used in the proof:

Lemma 1 (Nguyen et al. [43] with two variables). *Let \mathcal{X} and \mathcal{Y} be the sample spaces for X and Y , f be any function: $(\mathcal{X} \times \mathcal{Y}) \rightarrow \mathbb{R}$, and \mathcal{P} and \mathcal{Q} be the probability measures on $\mathcal{X} \times \mathcal{Y}$. Then,*

$$D_{\text{KL}}(\mathcal{P} \parallel \mathcal{Q}) = \sup_f \mathbb{E}_{(x,y) \sim \mathcal{P}}[f(x,y)] - \mathbb{E}_{(x,y) \sim \mathcal{Q}}[e^{f(x,y)}] + 1.$$

Proof. The second-order functional derivative of the objective is $-e^{f(x,y)} \cdot d\mathcal{Q}$, which is always negative. The negative second-order functional derivative implies the objective has a supreme value. Then, take the first-order functional derivative and set it to zero:

$$d\mathcal{P} - e^{f(x,y)} \cdot d\mathcal{Q} = 0.$$

We then get the optimal $f^*(x,y) = \log \frac{d\mathcal{P}}{d\mathcal{Q}}$. Plug in $f^*(x,y)$ into the objective, we obtain

$$\mathbb{E}_{\mathcal{P}}[f^*(x,y)] - \mathbb{E}_{\mathcal{Q}}[e^{f^*(x,y)}] + 1 = \mathbb{E}_{\mathcal{P}}[\log \frac{d\mathcal{P}}{d\mathcal{Q}}] = D_{\text{KL}}(\mathcal{P} \parallel \mathcal{Q}).$$

□

Lemma 2 (Nguyen et al. [43] with three variables). *Let \mathcal{X} , \mathcal{Y} , and \mathcal{Z} be the sample spaces for X , Y , and Z , f be any function: $(\mathcal{X} \times \mathcal{Y} \times \mathcal{Z}) \rightarrow \mathbb{R}$, and \mathcal{P} and \mathcal{Q} be the probability measures on $\mathcal{X} \times \mathcal{Y} \times \mathcal{Z}$. Then,*

$$D_{\text{KL}}(\mathcal{P} \parallel \mathcal{Q}) = \sup_f \mathbb{E}_{(x,y,z) \sim \mathcal{P}}[f(x,y,z)] - \mathbb{E}_{(x,y,z) \sim \mathcal{Q}}[e^{f(x,y,z)}] + 1.$$

Proof. The second-order functional derivative of the objective is $-e^{f(x,y,z)} \cdot d\mathcal{Q}$, which is always negative. The negative second-order functional derivative implies the objective has a supreme value. Then, take the first-order functional derivative and set it to zero:

$$d\mathcal{P} - e^{f(x,y,z)} \cdot d\mathcal{Q} = 0.$$

We then get the optimal $f^*(x,y,z) = \log \frac{d\mathcal{P}}{d\mathcal{Q}}$. Plug in $f^*(x,y,z)$ into the objective, we obtain

$$\mathbb{E}_{\mathcal{P}}[f^*(x,y,z)] - \mathbb{E}_{\mathcal{Q}}[e^{f^*(x,y,z)}] + 1 = \mathbb{E}_{\mathcal{P}}[\log \frac{d\mathcal{P}}{d\mathcal{Q}}] = D_{\text{KL}}(\mathcal{P} \parallel \mathcal{Q}).$$

□

A.1.1 Immediate results following Lemma 1

Lemma 3.

$$\begin{aligned} \text{Weak-CMI}(X; Y|Z) &= D_{\text{KL}}(P_{X,Y} \parallel \mathbb{E}_{P_Z} [P_{X|Z} P_{Y|Z}]) \\ &= \sup_f \mathbb{E}_{(x,y) \sim P_{X,Y}} [f(x,y)] - \mathbb{E}_{(x,y) \sim \mathbb{E}_{P_Z} [P_{X|Z} P_{Y|Z}]} [e^{f(x,y)}] + 1. \end{aligned}$$

Proof. Let \mathcal{P} be $P_{X,Y}$ and \mathcal{Q} be $\mathbb{E}_{P_Z} [P_{X|Z} P_{Y|Z}]$ in Lemma 1. □

Lemma 4. $\sup_f \mathbb{E}_{(x,y_1) \sim \mathcal{P}, (x,y_2:n) \sim \mathcal{Q}^{\otimes(n-1)}} \left[\log \frac{e^{f(x,y_1)}}{\frac{1}{n} \sum_{j=1}^n e^{f(x,y_j)}} \right] \leq D_{\text{KL}}(\mathcal{P} \parallel \mathcal{Q}).$

Proof. $\forall f$, we have

$$\begin{aligned}
D_{\text{KL}}(\mathcal{P} \parallel \mathcal{Q}) &= \mathbb{E}_{(x, y_{2:n}) \sim \mathcal{Q}^{\otimes(n-1)}} [D_{\text{KL}}(\mathcal{P} \parallel \mathcal{Q})] \\
&\geq \mathbb{E}_{(x, y_{2:n}) \sim \mathcal{Q}^{\otimes(n-1)}} \left[\mathbb{E}_{(x, y_1) \sim \mathcal{P}} \left[\log \frac{e^{f(x, y_1)}}{\frac{1}{n} \sum_{j=1}^n e^{f(x, y_j)}} \right] - \mathbb{E}_{(x, y_1) \sim \mathcal{Q}} \left[\frac{e^{f(x, y_1)}}{\frac{1}{n} \sum_{j=1}^n e^{f(x, y_j)}} \right] + 1 \right] \\
&= \mathbb{E}_{(x, y_{2:n}) \sim \mathcal{Q}^{\otimes(n-1)}} \left[\mathbb{E}_{(x, y_1) \sim \mathcal{P}} \left[\log \frac{e^{f(x, y_1)}}{\frac{1}{n} \sum_{j=1}^n e^{f(x, y_j)}} \right] - 1 + 1 \right] \\
&= \mathbb{E}_{(x, y_1) \sim \mathcal{P}, (x, y_{2:n}) \sim \mathcal{Q}^{\otimes(n-1)}} \left[\log \frac{e^{f(x, y_1)}}{\frac{1}{n} \sum_{j=1}^n e^{f(x, y_j)}} \right].
\end{aligned}$$

The first line comes from the fact that $D_{\text{KL}}(\mathcal{P} \parallel \mathcal{Q})$ is a constant. The second line comes from Lemma 1. The third line comes from the fact that (x, y_1) and $(x, y_{2:n})$ are interchangeable when they are all sampled from \mathcal{Q} .

To conclude, since the inequality works for all f , and hence

$$\sup_f \mathbb{E}_{(x, y_1) \sim \mathcal{P}, (x, y_{2:n}) \sim \mathcal{Q}^{\otimes(n-1)}} \left[\log \frac{e^{f(x, y_1)}}{\frac{1}{n} \sum_{j=1}^n e^{f(x, y_j)}} \right] \leq D_{\text{KL}}(\mathcal{P} \parallel \mathcal{Q}).$$

□

Note that Lemma 4 does not require $n \rightarrow \infty$, which is a much more practical setting compared to the analysis made only when $n \rightarrow \infty$. And a remark is that the equality holds in Lemma 4 when $n \rightarrow \infty$.

A.1.2 Immediate results following Lemma 2

Lemma 5.

$$\begin{aligned}
\text{CMI}(X; Y|Z) &= \mathbb{E}_{P_Z} [D_{\text{KL}}(P_{X, Y|Z} \parallel P_{X|Z} P_{Y|Z})] \\
&= D_{\text{KL}}(P_{X, Y, Z} \parallel P_Z P_{X|Z} P_{Y|Z}) \\
&= \sup_f \mathbb{E}_{(x, y, z) \sim P_{X, Y, Z}} [f(x, y, z)] - \mathbb{E}_{(x, y, z) \sim P_Z P_{X|Z} P_{Y|Z}} [e^{f(x, y, z)}] + 1.
\end{aligned}$$

Proof. Let \mathcal{P} be $P_{X, Y, Z}$ and \mathcal{Q} be $P_Z P_{X|Z} P_{Y|Z}$ in Lemma 2. □

A.1.3 Showing Weak-CMI $(X; Y|Z) \leq \text{CMI}(X; Y|Z)$

Proposition 6. *Weak-CMI* $(X; Y|Z) \leq \text{CMI}(X; Y|Z)$.

Proof. According to Lemma 3,

$$\begin{aligned}
\text{Weak-CMI}(X; Y|Z) &= \sup_f \mathbb{E}_{(x, y) \sim P_{X, Y}} [f(x, y)] - \mathbb{E}_{(x, y) \sim \mathbb{E}_{P_Z} [P_{X|Z} P_{Y|Z}]} [e^{f(x, y)}] + 1 \\
&= \sup_f \mathbb{E}_{(x, y, z) \sim P_{X, Y, Z}} [f(x, y)] - \mathbb{E}_{(x, y, z) \sim P_Z P_{X|Z} P_{Y|Z}} [e^{f(x, y)}] + 1.
\end{aligned}$$

Let $f_1^*(x, y)$ be the function when the equality for Weak-CMI $(X; Y|Z)$ holds, and let $f_2^*(x, y, z) = f_1^*(x, y)$ ($f_2^*(x, y, z)$ will not change $\forall z \sim P_Z$):

$$\begin{aligned}
\text{Weak-CMI}(X; Y|Z) &= \mathbb{E}_{(x, y, z) \sim P_{X, Y, Z}} [f_1^*(x, y)] - \mathbb{E}_{(x, y, z) \sim P_Z P_{X|Z} P_{Y|Z}} [e^{f_1^*(x, y)}] + 1 \\
&= \mathbb{E}_{(x, y, z) \sim P_{X, Y, Z}} [f_2^*(x, y, z)] - \mathbb{E}_{(x, y, z) \sim P_Z P_{X|Z} P_{Y|Z}} [e^{f_2^*(x, y, z)}] + 1.
\end{aligned}$$

Comparing the equation above to Lemma 5,

$$\text{CMI}(X; Y|Z) = \sup_f \mathbb{E}_{(x, y, z) \sim P_{X, Y, Z}} [f(x, y, z)] - \mathbb{E}_{(x, y, z) \sim P_Z P_{X|Z} P_{Y|Z}} [e^{f(x, y, z)}] + 1,$$

we conclude *Weak-CMI* $(X; Y|Z) \leq \text{CMI}(X; Y|Z)$. □

A.2 Proof of a tighter bound of $\text{CMI}(X; Y|Z)$

Next, we show a bound of $\text{CMI}(X; Y|Z)$ which is tighter than the proposed CCL. We term this bound as Tight-CCL.

Proposition 7 (A tighter bound of $\text{CMI}(X; Y|Z)$).

$$\begin{aligned} \text{Tight-CCL} &:= \sup_f \mathbb{E}_{z \sim P_Z} \left[\mathbb{E}_{(x_i, y_i) \sim P_{X, Y|z}^{\otimes n}} \left[\log \frac{e^{f(x_i, y_i, z)}}{\frac{1}{n} \sum_{j=1}^n e^{f(x_i, y_j, z)}} \right] \right] \\ &\leq \mathbb{E}_{P_Z} [D_{\text{KL}}(P_{X, Y|Z} \| P_{X|Z} P_{Y|Z})] = \text{CMI}(X; Y|Z), \end{aligned}$$

Proof. Given a $z \sim P_Z$, we let $\mathcal{P} = P_{X, Y|Z=z}$ and $\mathcal{Q} = P_{X|Z=z} P_{Y|Z=z}$. Then,

$$\mathbb{E}_{(x, y_1) \sim \mathcal{P}, (x, y_{2:n}) \sim \mathcal{Q}^{\otimes(n-1)}} \left[\log \frac{e^{f(x, y_1, z)}}{\frac{1}{n} \sum_{j=1}^n e^{f(x, y_j, z)}} \right] = \mathbb{E}_{(x_i, y_i) \sim P_{X, Y|z}^{\otimes n}} \left[\log \frac{e^{f(x_i, y_i, z)}}{\frac{1}{n} \sum_{j=1}^n e^{f(x_i, y_j, z)}} \right].$$

The only variables in the above equation are X and Y with Z being fixed at z , and hence the following can be obtained via Lemma 4:

$$\mathbb{E}_{(x_i, y_i) \sim P_{X, Y|z}^{\otimes n}} \left[\log \frac{e^{f(x_i, y_i, z)}}{\frac{1}{n} \sum_{j=1}^n e^{f(x_i, y_j, z)}} \right] \leq D_{\text{KL}}(\mathcal{P} \| \mathcal{Q}) = D_{\text{KL}}(P_{X, Y|Z=z} \| P_{X|Z=z} P_{Y|Z=z}).$$

The above inequality works for any function $f(\cdot, \cdot, \cdot)$ and any $z \sim P_Z$, and hence

$$\sup_f \mathbb{E}_{z \sim P_Z} \left[\mathbb{E}_{(x_i, y_i) \sim P_{X, Y|z}^{\otimes n}} \left[\log \frac{e^{f(x_i, y_i, z)}}{\frac{1}{n} \sum_{j=1}^n e^{f(x_i, y_j, z)}} \right] \right] \leq \mathbb{E}_{P_Z} [D_{\text{KL}}(P_{X, Y|Z} \| P_{X|Z} P_{Y|Z})].$$

□

We discuss the similarities and differences between CCL and Tight-CCL. Both are lower bounds of conditional mutual information $\text{CMI}(X; Y|Z)$, and both share formulations similar to InfoNCE [45]. The differences are that the scoring function $f(x, y, z)$ of Tight-CCL takes z as input, while CCL does not. Taking z as input makes Tight-CCL a tighter bound than CCL, which we show in Proposition 9. The reason we do not take z as an input in the CCL is because the sensitive attribute z in our setup is mostly binary, carries little information, and empirically Tight-CCL performs very similar to the proposed CCL (see Section B). CCL, on the other hand, has a simpler formulation and is easier to adapt to existing contrastive frameworks.

A.3 Proof of Equation (4) in the Main Text

Proposition 8 (Conditional Contrastive Learning (CCL), restating Equation (4) in the main text).

$$\begin{aligned} \text{CCL} &:= \sup_f \mathbb{E}_{z \sim P_Z} \left[\mathbb{E}_{(x_i, y_i) \sim P_{X, Y|z}^{\otimes n}} \left[\log \frac{e^{f(x_i, y_i)}}{\frac{1}{n} \sum_{j=1}^n e^{f(x_i, y_j)}} \right] \right] \\ &\leq D_{\text{KL}}(P_{X, Y} \| \mathbb{E}_{P_Z} [P_{X|Z} P_{Y|Z}]) = \text{Weak-CMI}(X; Y|Z) \leq \text{CMI}(X; Y|Z). \end{aligned}$$

Proof. By defining $\mathcal{P} = P_{X, Y}$ and $\mathcal{Q} = \mathbb{E}_{P_Z} [P_{X|Z} P_{Y|Z}]$, we have

$$\mathbb{E}_{(x, y_1) \sim \mathcal{P}, (x, y_{2:n}) \sim \mathcal{Q}^{\otimes(n-1)}} \left[\log \frac{e^{f(x, y_1)}}{\frac{1}{n} \sum_{j=1}^n e^{f(x, y_j)}} \right] = \mathbb{E}_{z \sim P_Z} \left[\mathbb{E}_{(x_i, y_i) \sim P_{X, Y|z}^{\otimes n}} \left[\log \frac{e^{f(x_i, y_i)}}{\frac{1}{n} \sum_{j=1}^n e^{f(x_i, y_j)}} \right] \right].$$

Via Lemma 4, we have

$$\sup_f \mathbb{E}_{z \sim P_Z} \left[\mathbb{E}_{(x_i, y_i) \sim P_{X, Y|z}^{\otimes n}} \left[\log \frac{e^{f(x_i, y_i)}}{\frac{1}{n} \sum_{j=1}^n e^{f(x_i, y_j)}} \right] \right] \leq D_{\text{KL}}(P_{X, Y} \| \mathbb{E}_{P_Z} [P_{X|Z} P_{Y|Z}]).$$

Combing with Proposition 6 that $\text{Weak-CMI}(X; Y|Z) \leq \text{CMI}(X; Y|Z)$, we conclude the proof. □

A.4 Showing CCL is a lower bound of Tight-CCL

Proposition 9.

$$\begin{aligned} \text{CCL} &:= \sup_f \mathbb{E}_{z \sim P_Z} \left[\mathbb{E}_{(x_i, y_i) \sim P_{X, Y|z}^{\otimes n}} \left[\log \frac{e^{f(x_i, y_i)}}{\frac{1}{n} \sum_{j=1}^n e^{f(x_i, y_j)}} \right] \right] \\ &\leq \text{Tight-CCL} := \sup_f \mathbb{E}_{z \sim P_Z} \left[\mathbb{E}_{(x_i, y_i) \sim P_{X, Y|z}^{\otimes n}} \left[\log \frac{e^{f(x_i, y_i, z)}}{\frac{1}{n} \sum_{j=1}^n e^{f(x_i, y_j, z)}} \right] \right]. \end{aligned}$$

Proof. Let $f_1^*(x, y)$ be the function when the equality holds in CCL, and let $f_2^*(x, y, z) = f_1^*(x, y)$ ($f_2^*(x, y, z)$ will not change $\forall z \sim P_Z$):

$$\text{CCL} := \mathbb{E}_{z \sim P_Z} \left[\mathbb{E}_{(x_i, y_i) \sim P_{X, Y|z}^{\otimes n}} \left[\log \frac{e^{f_2^*(x_i, y_i, z)}}{\frac{1}{n} \sum_{j=1}^n e^{f_2^*(x_i, y_j, z)}} \right] \right].$$

Since the equality holds with the supreme function in Tight-CCL, and hence

$$\text{CCL} \leq \text{Tight-CCL}.$$

□

B Experimental Details

B.1 Code

The code for this project will be updated soon.

B.2 Fairness Tabular Dataset Details

UCI Adult [16] focuses on predicting income of a person exceeds fifty thousand per year based on census data. It has a total of 48,842 samples, with a pre-determined training split of 32,561 samples and a test split of 16,281 samples. We choose the gender attribute as the sensitive attribute. It has the CC0: Public Domain License.

UCI German [16] focuses on predicting whether a person has good credit or not based on a set of attributes. It has a total of 10,00 samples. We follow the split in Ruoss et al. [51], where 80% of samples are drawn randomly and used as the training set and 20% samples are drawn randomly and used as the test set. We choose the age attribute as the sensitive attribute, which is determined by whether the individual's age exceeds a threshold. It has the Database Contents License v1.0.

UCI Crime: The Communities and Crime dataset [16] contains data including socioeconomic, law enforcement, and crime information for US communities. Specifically, it focuses on predicting whether a specific community is above or below the median number of violent crimes per population. It has 1,994 samples. We follow the split in Ruoss et al. [51], where 80% of samples are drawn randomly and used as the training set and 20% samples are drawn randomly and used as the test set. We choose the race attribute as the sensitive attribute, which is determined by whether the individual has race white. It has the Database Contents License v1.0.

COMPAS: The Recidivism Risk COMPAS Score dataset [1] contains a variety of demographic and crime information collected on the use of the COMPAS risk assessment tool in Broward County, Florida Angwin. It focuses on predicting recidivism (whether a criminal will reoffend or not) in the USA. It has 5,728 samples. We follow the split in Ruoss et al. [51], where 80% of samples are drawn randomly and used as the training set and 20% samples are drawn randomly and used as the test set. We choose the predefined binary race attribute as the sensitive attribute. It has the Database Contents License v1.0.

Law School: The Law School dataset is from the Law School Admission Study [64]. It has application records for 25 different law schools. It focuses on predicting whether a student passes the law school bar exam. It has 36,022 samples. We follow the split in Ruoss et al. [51], where 80% of

samples are drawn randomly and used as the training set and 20% samples are drawn randomly and used as the test set. We choose the race attribute as the sensitive attribute, which is determined by whether the individual has race white. It has the Database Contents License v1.0.

Dataset pre-processing : We perform the following types of preprocessing on all five fairness datasets: first, we standardize each numerical feature of the data to zero mean and unit variance. Next, we use one-hot encoding scheme for categorical features. Then, we drop rows and columns with missing values, and lastly we split into train, test and validation sets. For the contrastive pre-training, we augment each data sample using two noise vectors sampled from an isotropic Gaussian distribution, where the variance is a hyper-parameter. For the supervised fine-tuning, all downstream classification tasks are binary prediction tasks.

Personal identifiable information : Personally identifiable information is not available in all five datasets, because the authors of the datasets explicitly remove personal information when creating the datasets.

B.3 Vision Dataset Details

CelebA [39] is a human facial recognition dataset that contains more than 200,000 images of celebrity faces, where each facial image is annotated with 40 human-labeled binary attributes, including gender. Among the attributes, we select attractive, smile, and wavy hair and use them to form three separate binary classification tasks. The sensitive attribute is gender. The license of CelebA dataset claims that it is available for noncommercial research purposes only.

UTKFace [69] is a human facial recognition dataset that contains more than 20,000 images of human faces in a variety of age groups and races, where each facial image is annotated with three human-labeled binary attributes, including age, gender, and ethnicity. Among the attributes, we select age as the binary classification task (if the age of the individual is above a threshold). The sensitive attribute is the race attribute. The license of UTKFace dataset claims that it is available for noncommercial research purposes only.

Dataset pre-processing : For CelebA, we directly use the pre-defined training and test sets from the PyTorch data loader for CelebA. For UTKFace, we use a random 20% of all samples as the test set. The data augmentation details of both datasets will be included in Section B.5.

Personal identifiable information : Personally identifiable information is not available in the UTKFace data set, because the authors of the data sets explicitly remove personal information when creating the data set. For the CelebA dataset, each person has an ID, but the identity is not explicitly revealed (although users can infer the identities of some celebrities). Both datasets contain the annotated information, such as age, gender, and other facial attributes of the individuals in the images.

B.4 Fairness Tabular Dataset Training Details and Results

We follow the implementation from [51]. We use a three-layer neural network with hidden dimension 100 as the encoder and a linear layer as the fine-tuning network. We train 100 epochs and report the result. For pre-training, we use the Adam [34] optimizer, with a batch size of 256, a learning rate of 0.001, and a weight decay of 0.01. For fine-tuning, we use the same optimizer, batch size, weight decay, but a slightly larger learning rate 0.005.

Table 5: Accuracies and fairness results on five fairness datasets with confidence intervals. CCL has better downstream accuracy than existing unsupervised and self-supervised baselines in four datasets, and exhibits better fairness measurements in most cases.

	Model	Accuracy (%) (\uparrow)	Δ_{DP} (\downarrow)	Δ_{EO} (\downarrow)	$\Delta_{EO_{FP}}$ (\downarrow)
ADULT	Unsupervised				
	- LAFTR [41]	84.0	0.163	0.030	0.026
	- Ragonesi et al. [49]	85.0	-	0.030	-
	- DTM [35]	71.6	-	0.050	-
	- FNF [5]	80.0	0.110	-	-
	Self-Supervised				
	- FairMixRep [8]	85.0	0.172	-	-
	- SimCLR [9]	83.1 \pm 0.48	0.210 \pm 0.04	0.410 \pm 0.05	0.320 \pm 0.04
	- CCL (Ours)	85.4 \pm 0.53	0.110 \pm 0.02	0.070 \pm 0.01	0.090 \pm 0.01
- Tight-CCL (Ours)	85.3 \pm 0.48	0.108 \pm 0.03	0.068 \pm 0.01	0.093 \pm 0.01	
COMPAS	Unsupervised				
	- DTM [35]	66.0	-	0.200	-
	- FNF [5]	65.0	0.240	-	-
	Self-Supervised				
	- SimCLR [9]	71.2 \pm 0.33	0.103 \pm 0.01	0.227 \pm 0.06	0.134 \pm 0.04
	- CCL (Ours)	71.0 \pm 0.25	0.080 \pm 0.01	0.132 \pm 0.03	0.081 \pm 0.01
- Tight-CCL (Ours)	70.8 \pm 0.28	0.090 \pm 0.01	0.142 \pm 0.02	0.101 \pm 0.02	
CRIME	Unsupervised				
	- LCIFR [51]	84.4	0.443	0.314	0.212
	- FNF [5]	82.5	0.540	-	-
	Self-Supervised				
	- SimCLR [9]	82.1 \pm 0.32	0.502 \pm 0.08	0.530 \pm 0.02	0.383 \pm 0.01
	- CCL (Ours)	82.6 \pm 0.24	0.211 \pm 0.02	0.224 \pm 0.02	0.183 \pm 0.01
- Tight-CCL (Ours)	82.5 \pm 0.30	0.208 \pm 0.02	0.222 \pm 0.02	0.181 \pm 0.02	
GERMAN	Unsupervised				
	- LCIFR [51]	73.1	0.102	0.080	0.063
	- Ragonesi et al. [49]	74.0	-	0.060	-
	Self-Supervised				
	- FairMixRep [8]	71.8	0.089	-	-
	- SimCLR [9]	72.5 \pm 0.11	0.250 \pm 0.05	0.382 \pm 0.06	0.195 \pm 0.04
- CCL (Ours)	74.3 \pm 0.28	0.083 \pm 0.01	0.128 \pm 0.03	0.062 \pm 0.01	
- Tight-CCL (Ours)	74.4 \pm 0.25	0.085 \pm 0.01	0.126 \pm 0.02	0.062 \pm 0.01	
LAW SCHOOL	Unsupervised				
	- LCIFR [51]	84.4	0.110	0.180	0.070
	- FNF [5]	84.6	0.050	-	-
	Self-Supervised				
	- SimCLR [9]	83.6 \pm 0.54	0.086 \pm 0.02	0.212 \pm 0.04	0.110 \pm 0.02
	- CCL (Ours)	84.8 \pm 0.50	0.051 \pm 0.01	0.153 \pm 0.03	0.056 \pm 0.01
- Tight-CCL (Ours)	84.5 \pm 0.44	0.050 \pm 0.01	0.150 \pm 0.02	0.055 \pm 0.01	

Results. We include the results in Table 5. All entries with – indicate that the corresponding metrics are not reported in the original papers. The following results are read off from the figures in the paper: LAFTR [41], DTM [35], and FNF [5]. We include the confidence intervals of the results, and bold the entries that have overlapping confidence intervals with the best performing entries in that dataset. SimCLR is a re-implementation of Chen et al. [9] on the new datasets. Tight-CCL represents a tighter bound of conditional mutual information, which is introduced and discussed in Proposition 7. From the results, we can conclude that CCL outperforms all baselines on eleven out of the eighteen fairness metrics. Also, CCL outperforms all baselines on downstream accuracy on four out of five datasets. We note that Tight-CCL performs very close to CCL, sometimes better than CCL in terms of fairness metrics. This may be due to that the Tight-CCL is a tighter bound of conditional mutual information, and optimizing Tight-CCL leads to a representation closer to conditional mutual information maximization. Because conditional mutual information explicitly excludes information from the sensitive attribute Z , Tight-CCL is able to remove slightly more effect from the sensitive attribute than CCL. We use CCL in the main text as it has a simpler formulation and is easier to adapt to existing contrastive frameworks.

Computational resource We perform all experiments on a single GeForce RTX 2080 Ti GPU and a 32-core Intel CPU processor. Training 100 epochs in different datasets vary based on the size of the dataset, but the overall training time of 100 epochs on one dataset is below an hour.

B.5 Vision Dataset Training Details and Results

We follow the implementation from [9]. We use a ResNet-50 as the encoder and a two-layer network with hidden dimension 512 as the fine-tuning network. We train 100 epochs and report the result. For the contrastive pre-training, we use the Adam [34] optimizer, with a batch size of 256, a learning rate of 0.0003, and a weight decay of 10^{-6} . For the supervised fine-tuning, we use the same optimizer, batch size, weight decay, but a slightly larger learning rate 0.001.

Table 6: Accuracies and fairness results on two vision datasets on four prediction tasks with confidence intervals. Best results are bold. CCL has better downstream accuracy in all four tasks, and exhibits better or close-to-the-best fairness measurements in 11 out of 12 results.

	Model	Accuracy (%) (\uparrow)	Δ_{DP} (\downarrow)	Δ_{EO} (\downarrow)	$\Delta_{EO_{FP}}$ (\downarrow)
CELEBA ATTRACTIVE	Unsupervised				
	- MFD [30]	80.2	-	0.050	-
	- Balunovic et al. [5]	79.4	-	0.238	-
	- Morales et al. [42]	77.7	-	0.070	-
	Self-Supervised				
	- SimCLR [9]	81.7 \pm 0.32	0.277 \pm 0.04	0.212 \pm 0.03	0.110 \pm 0.01
	- CCL (Ours)	82.1 \pm 0.24	0.202 \pm 0.03	0.101 \pm 0.01	0.048 \pm 0.01
- Tight-CCL (Ours)	81.9 \pm 0.33	0.200 \pm 0.02	0.106 \pm 0.02	0.052 \pm 0.01	
CELEBA WAVY HAIR	Unsupervised				
	- FactorVAE [33]	64.5	-	0.388	0.288
	- FFVAE [13]	61.0	-	0.211	0.154
	Self-Supervised				
	- SimCLR [9]	67.7 \pm 0.76	0.403 \pm 0.05	0.355 \pm 0.04	0.210 \pm 0.02
	- CCL (Ours)	67.7 \pm 0.69	0.202 \pm 0.02	0.189 \pm 0.02	0.102 \pm 0.01
- Tight-CCL (Ours)	67.8 \pm 0.44	0.198 \pm 0.03	0.172 \pm 0.02	0.093 \pm 0.01	
CELEBA SMILE	Unsupervised				
	- Morales et al. [42]	88.4	-	0.060	-
	Self-Supervised				
	- SimCLR [9]	89.3 \pm 0.33	0.102 \pm 0.01	0.142 \pm 0.01	0.078 \pm 0.01
	- CCL (Ours)	89.7 \pm 0.25	0.086 \pm 0.01	0.060 \pm 0.01	0.053 \pm 0.01
- Tight-CCL (Ours)	89.5 \pm 0.27	0.084 \pm 0.01	0.060 \pm 0.01	0.056 \pm 0.01	
UTKFACE GENDER	Unsupervised				
	- AD [67]	74.7	-	0.204	-
	- MFD [30]	74.7	-	0.178	-
	Self-Supervised				
	- SimCLR [9]	78.0 \pm 0.25	0.335 \pm 0.03	0.421 \pm 0.04	0.287 \pm 0.03
	- CCL (Ours)	78.5 \pm 0.22	0.191 \pm 0.02	0.156 \pm 0.02	0.089 \pm 0.01
- Tight-CCL (Ours)	78.3 \pm 0.15	0.188 \pm 0.02	0.159 \pm 0.02	0.110 \pm 0.02	

Results. We include the results in Table 6. All entries with – indicate that the corresponding metrics are not reported in the original papers. We include the confidence intervals of the results, and bold the entries that have overlapping confidence intervals with the best performing entries in that dataset. Similar to our observation in Section B.4, from the results we can conclude that CCL outperforms all baselines on eleven out of the twelve fairness metrics. Also, CCL outperforms all baselines on downstream accuracy on all four tasks. Tight-CCL also performs very close to CCL, although some downstream task performances of Tight-CCL is slightly worse than that of CCL.

Computational resource We perform all experiments on a single GeForce RTX 2080 Ti GPU and a 32-core Intel CPU processor. Training 100 epochs on CelebA or UTKFace takes approximately 20 – 24 hours, depending on the server’s condition.